OPEN ACCESS

PRZEGLĄD ELEKTROTECHNICZNY

Adam MUC[1], Andrzej KASPROWICZ[2]
ORCID: [1]0000-0002-9495-087X; [2]0000-0001-7614-2724
DOI: 10.15199/48.2025.11.24

Control concept of a 6-phase asynchronous motor using a 3-phase inverter and magnetically coupled chokes

Koncepcja sterowania 6-fazowym silnikiem asynchronicznym przez falownik 3-fazowy i dławiki sprzężone magnetycznie

[1] dr inż. Adam Muc, Uniwersytet Morski w Gdyni, Wydział Elektrotechnik, ul. Morska 81–87, 81-225 Gdynia,
E-mail: a.muc@we.umg.edu.pl
[2] dr inż. Andrzej Kasprowicz, Uniwersytet Morski w Gdyni, Wydział Elektrotechnik, ul. Morska 81–87, 81-225 Gdynia,
E-mail.a.kasprowicz@we.umg.edu.pl.

Correspondence address: a.muc@we.umg.edu.pl

Abstract. The article presents the possibility of controlling a 6-phase asynchronous induction motor by a 3-phase inverter. The scalar algorithm U/f=constant was used to control the inverter, while the 3-phase voltage system obtained in this way was transferred to a 6-phase motor using magnetically coupled chokes in the TDS system. An important element of the article is the experimental research carried out with and without the motor loaded at different speeds. The obtained results confirm the reasonable use of such a power supply system in the case of a 6-phase motor and, at the same time, indicate the limitations that accompany it.

Keywords: 6-phase motor, magnetically coupled chokes, scalar control

Streszczenie. W artykule przedstawiono możliwość sterowania 6-fazowym indukcyjnym silnikiem asynchronicznym przez falownik 3-fazowy. Do sterowania falownikiem wykorzystano algorytm skalarnym U/f = constans, natomiast otrzymany w ten sposób 3-fazowy układ napięć przeniesiono na silnik 6 fazowy za pomocą dławików sprzężonych magnetycznie w układzie TDS. Istotnym elementem artykułu są badania eksperymentalne przeprowadzone przy obciążeniu silnika i jego braku oraz różnych prędkościach pracy silnika. Uzyskane wyniki potwierdzają zasadne zastosowanie takiego systemu zasilania w przypadku silnika 6-fazowego i jednocześnie wskazują na ograniczenia, które temu towarzyszą.

Słowa kluczowe: silnik 6-fazowy, dławiki sprzężone magnetycznie, sterowanie skalarne

Introduction

Induction motors (IMs) dominate the electric machine market, accounting for approximately 70% of applications, mainly due to their robustness, cost-effectiveness, and compatibility with both direct grid and inverter operation [1, 2]. While standard IMs are typically three-phase, six-phase induction motors (6PIMs) have gained attention for their enhanced torque density, fault tolerance, and reduced core losses [3, 4, 5, 6].

Recent studies highlight the industrial relevance of multiphase machines, especially in high-demand applications like pumps and compressors [7]. Six-phase configurations are particularly attractive because they can be implemented by rewinding conventional three-phase stator frames [8]. Comparative analyses demonstrate superior performance of 6PIMs over three-phase machines in terms of torque, speed stability, and efficiency [1, 9–11].

However, 6PIMs require more complex and costly drive systems, including a six-phase inverter and dedicated control algorithms [12–15]. Among control strategies, the scalar V/F method remains popular due to its simplicity and suitability for various applications [16–19]. The advanced control methods, such as flux vector and sensorless vector control, are also explored for performance optimization [20, 21].

Phase conversion is critical in high-current scenarios (e.g., induction furnaces), where six-phase systems are derived from three-phase supplies using specialized transformers [22–25].

The paper [26] proposes a drive system for a modified six-phase IM suitable for both variable and constant speed applications. The motor is supplied by a standard three-phase inverter combined with a three-to-six-phase transformer. A scalar closed-loop V/F control is implemented for variable speed, whereas for constant speed, the transformer alone suffices.

The article presents the possibility of controlling a 6-phase asynchronous induction motor by a 3-phase inverter. The scalar algorithm U/f=constants was used to control the inverter, while the 3-phase voltage system obtained in this way was transferred to a 6-phase motor using magnetically coupled chokes in the TDS system. An important element of the article is the experimental research carried out with and without the motor loaded at different speeds. The obtained results confirm the reasonable use of such a power supply system in the case of a 6-phase motor and, at the same time, indicate the limitations that accompany it.

Power supply and control system

Figure 1 shows a system that enables a 6-phase induction motor to be controlled and powered by a 3-phase voltage inverter implementing the U/f = constant scalar algorithm. The presented control and power system consists of a power source with an intermediate circuit, a 3-phase voltage inverter, magnetically coupled chokes connected in a TDS circuit, a 6-phase induction motor, and a microprocessor controller.

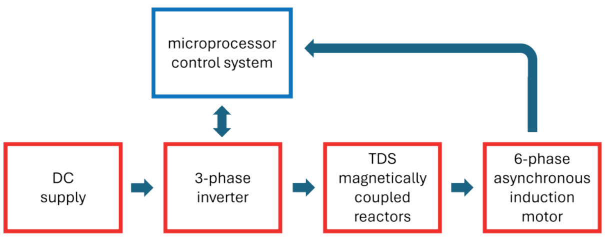

Fig. 1. Schematic diagram of the power supply system for a 6-phase induction motor by a 3-phase inverter and magnetically coupled reactors

Figure 2 shows the wiring diagram of the magnetically coupled chokes in the TDS system.

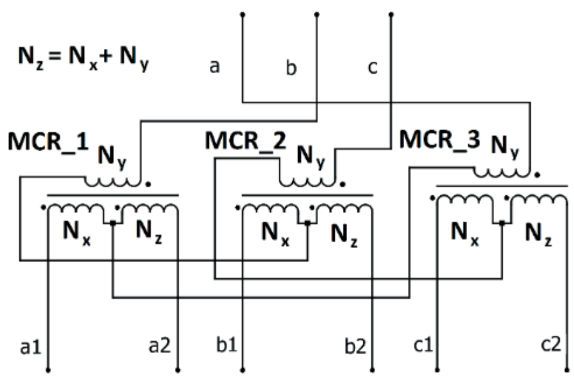

Fig. 2. Schematic of magnetically coupled chokes in TDS, where: N_x, N_y and N_z – the number of turns of the inductances used

The experiment used an available magnetically coupled choke system, which had the following parameters: Nx: Ny: Nz = 2.72:1:3.72. It was used in the studies described in [27, 28], in which a 12-plus controlled rectifier and the second converter-inverter with multiple DC inputs were developed and studied.

The scalar control algorithm of the inverter implemented the strategy U/f = constant. (Figure 3). The supply voltage U of the inverter was reduced to 240 (V). Scalar U/f control is widely used in various industrial applications such as air conditioning and ventilation. It was also used almost unchanged in the work [29]. In the contemplated case, the U/f ratio was equal to 4. The choice of the ratio was guided by the fact that with a reduced supply voltage and a rated frequency equal to f_N = 50 (Hz), the control did not enter the range of overmodulation. The reduction of the supply voltage in the intermediate circuit, on the other hand, was due to the possibility of an available DC voltage source. The control algorithm was implemented in the PLECS 4.8.10 (64-bit) software environment. The software used made it possible to both simulate the circuit with the control and generate the code that controls the experimental circuit. A module called CODER available in the PLECS program was used for code generation. In the experimental study, LaunchPad XL VER was used to control the converter. 2.0 with a microcontroller of the C2000 TMS320F2879D family. The microcontroller implemented the U/f=constant control algorithm in real time with an interrupt cycle of ts = 50 (μs). At the same time, the angular velocity of the motor was measured with a quadrature encoder with a pulse count of 2048 (pulses/rev), motor currents and voltage Udc. The load of the microcontroller was monitored and was about 38%.

The control algorithm itself is not the purpose of the paper, so it is presented in a limited way.

Laboratory workstation

The laboratory bench where the tests were performed is shown in Figure (4a) and (4b). Figure 4a shows a cabinet with inverter (1), intermediate circuit and power supply (2). Figure 4b shows the drive unit with connected measuring courts (3) and magnetically coupled chokes (4).

Measurements were recorded with a DPO7054 oscilloscope using current probes TCP0150 and P5210 voltage probes. The current and voltage waveforms were then analyzed for higher harmonic content using oscilloscope programming.

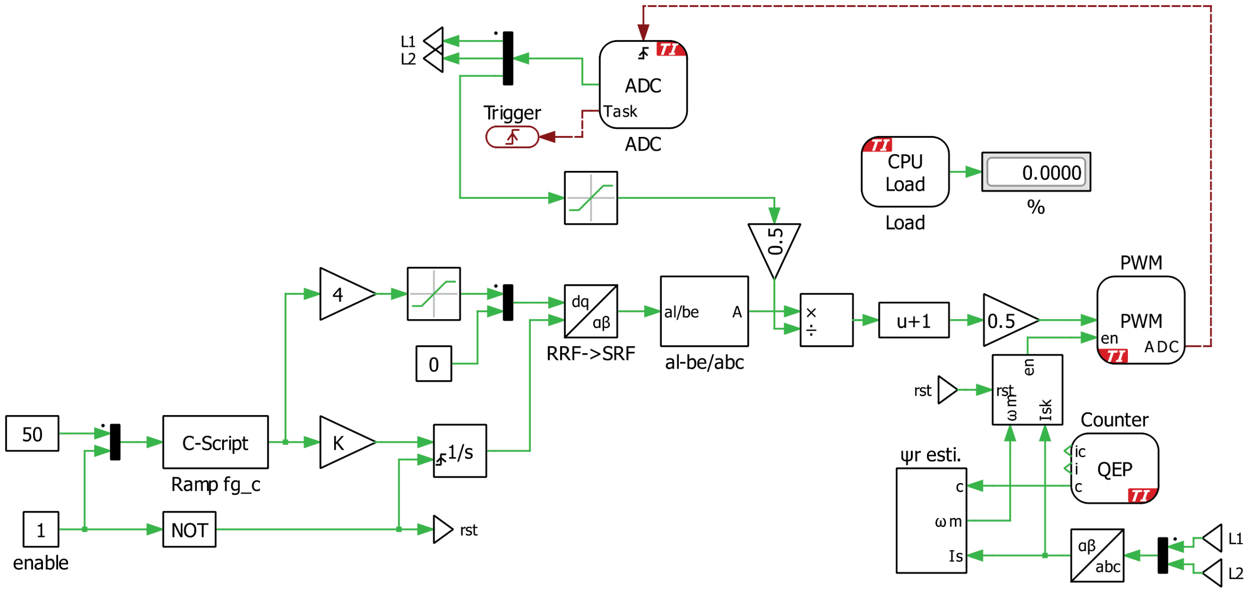

Fig. 3. Block diagram of the U/f scalar control algorithm

Fig. 4a. View of cabinet with inverter (1), intermediate circuit and power supply (2).

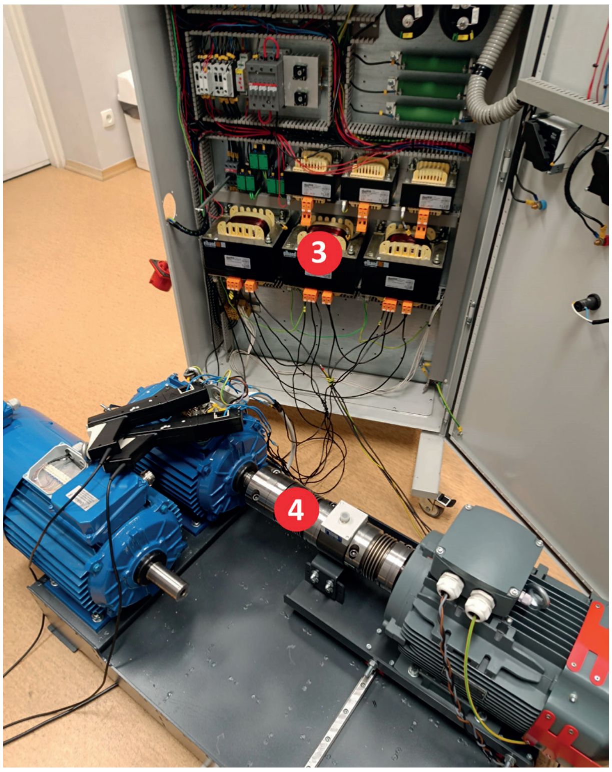

Fig. 4b. View of the drive unit with connected measuring courts (3) and magnetically coupled chokes (4)

The asynchronous induction motor number 6Sg132S4 was used in the tests. The most important motor parameters are: power $P_n = 4$ (kW), voltage $U_n = 400$ (V), current $I_n = 4.7$ (A), frequency $f_n = 50$ (Hz), speed $n_n = 1472$ rpm, connection system YY/30°, efficiency $\eta_n = 87\%$.

Experimental studies

The plan for the experimental studies included measuring voltages and currents and calculating the spectrum for a 6-phase motor operating at idle and with a load. The tests were performed for different modulating frequencies, i.e., 20 Hz, 30 Hz, 40 Hz, and

50 Hz, which translated into the speeds at which the motor operated.

Figures 5 and 6 present the phase voltage waveforms (u_{a1}, u_{a2}) and phase current waveforms (i_{a1}, i_{a2}). The voltage waveforms exhibit identical amplitude values under both no-load and load conditions. Conversely, a distinct difference is observed in the phase current waveforms (i_{a1} and i_{a2}) when comparing no-load and load operation. A noticeable discrepancy in the peak current values is evident, with the difference being more pronounced between no-load and load states. Under load conditions, the phase currents tend to amplitude equalization, and the phase displacement between them approaches 30°.

Figures 7 and 8 present characteristics that show the change in phase angle between currents ia1 and ia2 as a function of modulating frequency at no load and with a load representing 20% of the nominal load value of the motor under test.

The characteristics presented in Figures 7 and 8 indicate an important feature of the system, which simultaneously constitutes its limitation, namely that for

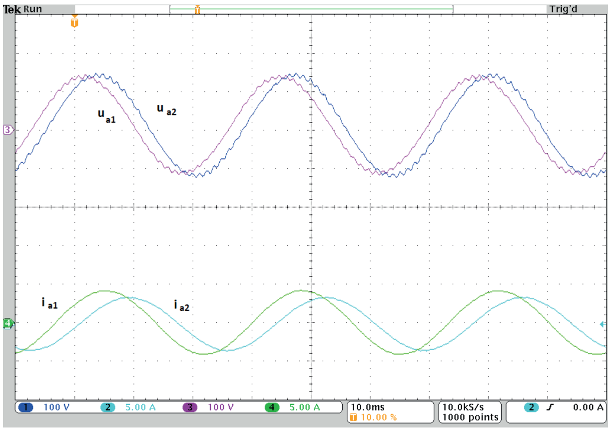

Fig. 5. Oscillogram of voltage and current waveforms recorded during no-load motor operation, where u_{a1} and u_{a2} denote phase voltages, and i_{a1} and i_{a2} denote phase currents.

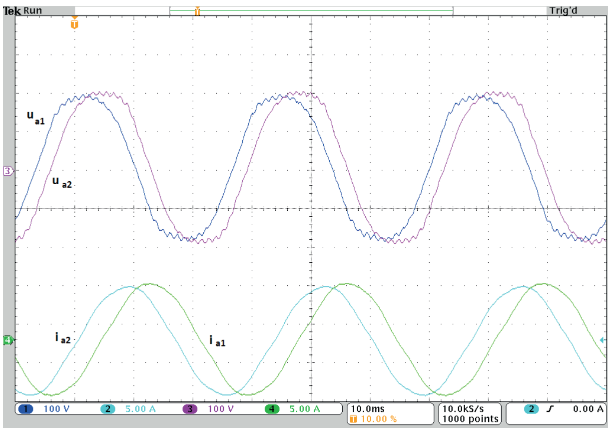

Fig. 6. Oscillogram of voltage and current waveforms recorded during motor operation under load, where u_{a1} and u_{a2} denote phase voltages, and i_{a1} and i_{a2} denote phase currents.

the proper operation of magnetically coupled inductors, it is necessary to load the inductors with a current of sufficient magnitude to achieve the appropriate phase angle between the output currents.

Additional insights into the influence of load and no-load conditions on the operation of a system dominated by coupled inductors are provided by the characteristic shown in Figure 9.

The results presented in Figure 9 confirm the previous observation, namely that the phase shift between the currents under no-load conditions is significantly smaller, resulting in a greater difference between the current amplitude values. When the system is loaded, the phase angle between the currents increases, leading to a decrease in the amplitude difference, with the currents tending to equalize.

This observation is further supported by the characteristic shown in Figure 10, which presents the variation of the amplitudes of currents ia1 and ia2 as a function of the load. As the load increases, the current amplitudes also increase, and the difference between them gradually diminishes.

The characteristic shown in Figure 11 presents the variation of the phase shift as a function of load under a constant modulation frequency in the U/f control algorithm. As the load increases, the current flowing

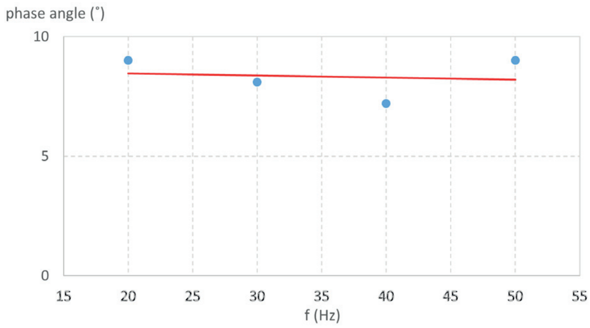

Fig. 7. The characteristic shows the variation of the phase angle between currents i_{a1} and i_{a2} as a function of the modulation frequency under no-load conditions

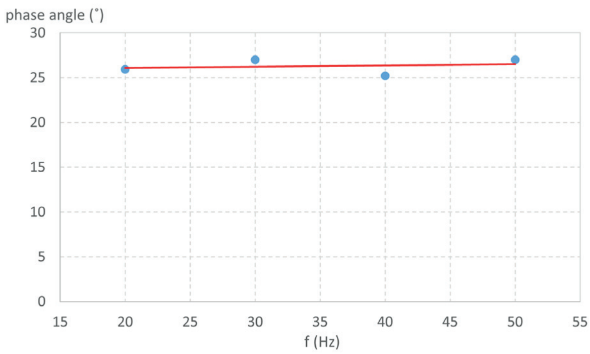

Fig. 8. The characteristic shows the variation of the phase angle between currents i_{a1} and i_{a2} as a function of the modulation frequency under constant load conditions.

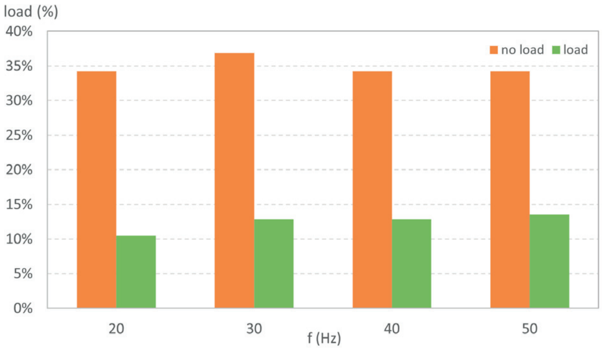

Fig. 9. Percentage change in the amplitudes of currents i_{a1} and i_{a2} under no-load and load conditions

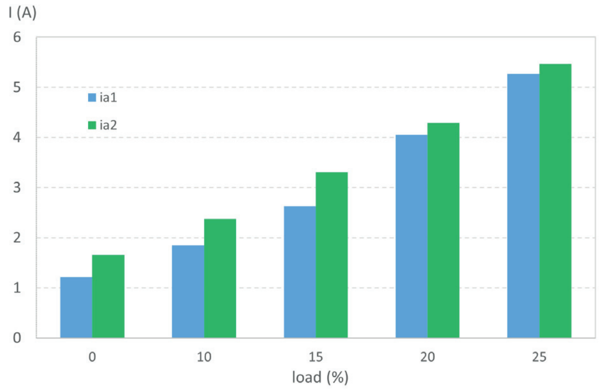

Fig. 10. Percentage change in the amplitudes of currents i_{a1} and i_{a2} with increasing load

through the inductors rises, causing the inductors to couple in such a way that the currents between terminals a1 and ab (see Fig. 2) shift relative to each other by an angle approaching 30°.

Conclusion

The article presents the possibility of supplying and controlling a six-phase induction motor using a three-phase inverter. Magnetically coupled inductors in a TDS configuration were used as the system for converting three phases into six phases. Similar solutions were proposed in [26]; however, in that case, the phase transformation system consisted of three interconnected transformers. Compared to transformers, inductors mainly differ in that, for the same power rating, their size and weight are significantly smaller, as discussed in [27, 28].

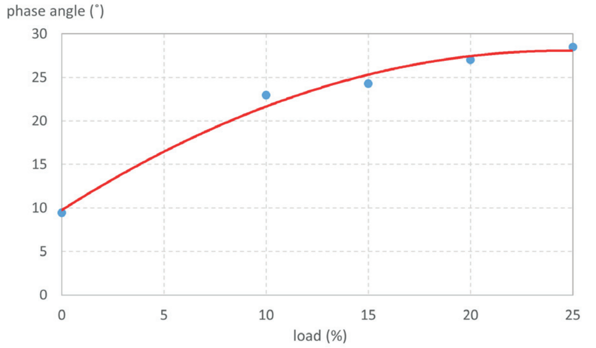

Fig. 11. The characteristic shows the variation of the phase angle as a function of load at a constant modulation frequency of 30 Hz

The proposed method of supplying a six-phase motor appears attractive primarily due to the fact that complex control algorithms, whose complexity increases with the number of phases, are not required. Another advantage is that a standard three-phase inverter can still be used, which is easier to control than a six-phase inverter. Typically, a six-phase inverter is obtained by combining two three-phase inverters, which, in simple terms, results in approximately double the inverter cost. The magnetically coupled inductors used are passive components, and therefore exhibit low failure rates and low susceptibility to damage.

However, it is important to point out a significant limitation of this solution, namely the necessity of ensuring an appropriate load on the inductors to achieve a 30° phase shift between the currents, which is not possible during no-load motor operation. As a consequence, if the motor operates under improper loading conditions, the current amplitudes will not be equal, which may affect motor performance and, in particular, could become a source of vibrations. In this respect, the described system requires further investigation. Inadequate loading may also result in the six-phase motor operating similarly to a three-phase motor, which would represent a major disadvantage of this solution.

Received: 05.10.2025, **Accepted:** 04.11.2025, **Published:** 24.11.2025

REFERENCES

[1] Sahin A.D., Yaldiz E., Modeling and analysis of induction motors, Energy, 2021.
[2] Rashed M., et al., Induction motor control using voltage source inverters, IEEE Trans. Ind. Appl., 2020.
[3] Nandi S., et al., A review of fault-tolerant multiphase induction motors, IEEE Trans. Ind. Electron., 2020.
[4] Tapia J.A., Asher G.M., Industrial applications of multiphase machines, IEEE Ind. Appl. Mag., 2019.
[5] Piepenbreier B., Kaltenbach K., Multiphase drives in pump systems, Proc. EPE Conf., 2020.
[6] El-Refaie A.M., Benefits of multiphase machines for industrial applications, IEEE Trans. Ind. Electron., 2021.

[7] Abu-Rub H., et al., Six-phase motor drives for compressors, Energies, 2021.
[8] Jones R., et al., Conversion of three-phase stators to six-phase configuration, IEEE Trans. Energy Convers., 2021.
[9] Sutikno T., et al., Performance comparison of 3-phase and 6-phase IMs, J. Electr. Eng. Technol., 2020.
[10] Camara M.B., et al., Torque analysis in six-phase IMs, IEEE Trans. Ind. Appl., 2021.
[11] Beig A.R., et al., Core loss reduction in multiphase machines, IEEE Trans. Magn., 2020.
[12] Gerada C., et al., Design challenges for six-phase inverters, IEEE Trans. Ind. Electron., 2021.
[13] Xu L., Wu B., Control techniques for multiphase drives, IEEE Trans. Power Electron., 2019.
[14] Vas P., Sensorless Vector and Direct Torque Control, Oxford University Press, 2020.
[15] Barrero F., Duran M.J., Multiphase drives: Control strategies, IEEE Ind. Electron. Mag., 2021.
[16] Bowes S.R., Midya A., Scalar control of induction machines, IEE Proc. Electr. Power Appl., 2020.
[17] Bose B.K., Modern Power Electronics and AC Drives, Prentice Hall, 2021.
[18] Tripathi A., Jain S.K., V/f control for high-performance induction motor drive, Energy Reports, 2021.
[19] Mondal S.K., et al., Closed-loop scalar control of IMs, IEEE Trans. Ind. Electron., 2020.
[20] Pellegrino G., et al., Flux vector control of multiphase drives, IEEE Trans. Ind. Appl., 2021.
[21] Kim Y.S., Lee H.W., Sensorless vector control for six-phase motors, IEEE Trans. Power Electron., 2020.
[22] Krishnaswami H., Mohan N., Three-phase to six-phase AC conversion for IM drives, IEEE Trans. Power Electron., 2020.
[23] Gupta A.K., et al., Transformer design for multiphase systems, IEEE Trans. Ind. Electron., 2021.
[24] Holtz J., Oikonomou N., Six-phase supply from three-phase transformers, Proc. IECON, 2020.
[25] Krishnan R., Electric Motor Drives: Modeling, Analysis, and Control, Prentice Hall, 2020.
[26] Abdelwanis, M.I., Rashad, E.M., Taha, I.B.M., Selim, F.F., Implementation and Control of Six-Phase Induction Motor Driven by a Three-Phase Supply. Energies 2021, 14, 7798. https://doi.org/10.3390/en14227798
[27] Muc A., „The Three-Phase Converter with Configurable DC Input and Multilevel AC Output, " 2024 IEEE 18th International Conference on Compatibility, Power Electronics and Power Engineering (CPE-POWERENG), Gdynia, Poland, 2024, pp. 1–6, doi: 10.1109/CPE-POWERENG60842.2024.10604391
[28] Muc A., Kasprowicz A., Bielecka A., Mysiak P., Iwaszkiewicz J., „The Twelve-Pulse Controlled Rectifier with Magnetically Coupled Reactors for Powering Marine Electrical Equipment, " 2024 IEEE 18th International Conference on Compatibility, Power Electronics and Power Engineering (CPE-POWERENG), Gdynia, Poland, 2024, pp. 1–6, doi: 10.1109/CPE-POWERENG60842.2024.10604382
[29] Downar-Zapolski M., Kasprowicz A., Projekt laboratoryjnego falownika 3-fazowego sterowanego przy użyciu środowiska symulacyjnego PLECS, Przegląd Elektrotechniczny, ISSN 0033–2097, R. 99 NR 11/2023